

Joint intensity in layered rocks: The unsaturated, saturated, supersaturated, and clustered classes

Amir Sagy* and Ze'ev Reches†

Institute of Earth Sciences, The Hebrew University of Jerusalem, Jerusalem 91904, Israel

(Received 5 January 2005; accepted in revised form 12 September 2005)

ABSTRACT

Sagy, A. and Reches, Z. 2006. Joint intensity in layered rocks: The unsaturated, saturated, supersaturated, and clustered classes. *Isr. J. Earth Sci.* 55: 33–42.

We derive here a new model for joint intensity in brittle, layered rock. According to this model, joint intensity depends on the tectonic stresses, the friction between the layers, and the tensile strength of the brittle layers. For typical geological settings of layered sedimentary rocks, the joint intensity is expected to achieve saturation when the ratio of the host layer thicknesses to the joint spacing ranges from 1 to 3. On the other hand, field measurements in the western margins of the Dead Sea basin, as well as experimental observations, reveal that this ratio ranges from 0.1 to 35. Consequently, we classify the observed range of intensity into four groups: unsaturated, saturated, supersaturated, and clustered. While our model, as well as previous models, can explain the first two groups, alternative mechanisms are required to explain the second two groups. It is shown, based on our recent field and experimental analyses, that fast propagating, dynamic fractures can produce the tightly spaced patterns of the supersaturated and clustered cases.

INTRODUCTION

The occurrence of fractures in sedimentary rocks strongly affects the mechanical and hydrological properties of the host layers. The fracture intensity in three dimensions is the cumulative surface area of fractures within a unit volume; this value has never been determined. As a two-dimensional approximation, fracture intensity can be determined by measuring the cumulative length of fractures (map view) per unit area of a map (Wu and Pollard, 1995; Reches, 1998; Sagy, 1999). Many times, however, fracture intensity is estimated from a one-dimensional traverse (scan-line) normal to the fractures.

Several field studies (e.g., Narr and Suppe, 1991; Gross, 1993; Engelder et al., 1997; Ji et al., 1998)

demonstrated that mean or median joint spacing (S) in layered rocks is often linearly related to layer thickness (h); joint (or fracture) intensity is defined as $D = h/S$. Mechanical models predict that the layer can become “saturated” with joints, and that at this stage new joints cannot form (Ji et al., 1998; Bai and Pollard, 2000). Other field studies, however, display a different picture. It has been shown that the intensity of joints can vary widely, from sparse occurrence to tight spacing, and in these cases there is a nonlinear relationship

*Current address: Department of Earth and Space Sciences, University of California, Los Angeles CA 90095-1567, USA. E-mail: asagy@moho.ess.ucla.edu

†Current Address: School of Geology and Geophysics, University of Oklahoma, Norman, OK 73072, USA.

between the joint spacing and the layer thickness (Reches, 1972, 1998; McQuillan, 1973; Ladeira and Price, 1981; Sagy et al., 2001).

The present study uses field observations from the western margins of the Dead Sea basin and experimental observations to explore two different mechanisms that control joint intensity in layered rocks. One mechanism, which is based on quasi-static fracturing within brittle layers, predicts a linear relationship between the layer thicknesses, and that the saturation intensity D_s is smaller than 3; D_s is the ratio of the final fracture spacing to the thickness of the host layer. While this mechanism is in agreement with observations in many studies (e.g., Price, 1966; Hobbs, 1967; Sowers, 1973; Gross et al., 1995; Ji et al., 1998; Sagy, 1999; Bai and Pollard, 2000), it fails to explain the high joint intensity of $D \gg 3$ found in other sites. The second mechanism is based on nonlinear processes during fast propagation of dynamic fractures (Sharon and Fineberg, 1996; Sagy et al., 2001, 2004). We follow here the common practice and use “fracture” for tensile, mode I fractures in models and experiments, and the term “joints” for tensile fractures in the field.

MODELING JOINT INTENSITY IN LAYERED ROCKS

Basic concepts

Fracturing models are usually based on a two-dimensional view of alternating brittle and ductile layers (Fig. 1). The strength of the contacts between the layers is assumed to be due to the bonding between elastic or viscoelastic solids (Price, 1966; Hobbs, 1967; Sowers, 1973; Gross et al., 1995; Bai and Pollard, 2000), controlled by pore fluid pressure (Ladeira and Price, 1981), or caused by friction (Ji et al., 1998; Sagy, 1999). These analyses assume, explicitly or implicitly, that the fractures grow by slow, quasi-static extension.

Hobbs (1967) considered fracturing within a layered sequence subjected to layer-parallel extension (Fig. 1). A fracture forms in the brittle layer when the local tensile stresses exceed the tensile strength of this layer. The formation of this fracture relaxes the tensile stresses at its proximity, thus reducing the likelihood for a new fracture to ensue and grow. Shear stresses along the layer contacts transfer extension from the ductile layers to the brittle one, and the tensile stress increases with distance from the fracture. The brittle layer fractures again wherever the tensile stress exceeds the local strength. Hobbs' (1967) model and its

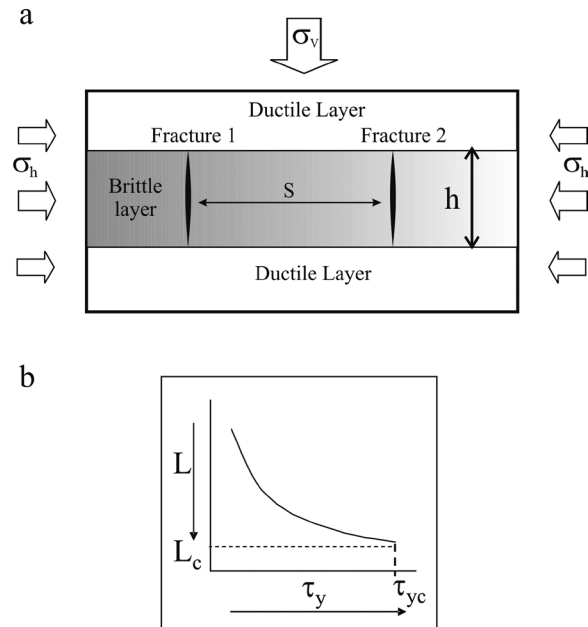


Fig. 1. (a) A two-dimensional section of a fractured brittle layer between two ductile layers. h —thickness of the brittle layer; S —the spacing between joints; σ_v and σ_h are remote stresses in extensional tectonic regime. (b) The dependence of the distance between joints (S) on the increasing shear stress (τ_y) is conceptually demonstrated, following Kelly and Tyson (1965). The fracturing process within the brittle material will stop at S_c (eq 2) when the shear stress required to create new fractures in the brittle material is equal to the shear strength of the contacts (τ_{yc}).

offsprings predict that fracture intensity is proportional to the layer-parallel extension and stress intensity in the ductile (less competent) layers (Kelly and Tyson, 1965; Gross et al., 1995).

The saturation intensity can be estimated for known rock properties. Bai and Pollard (2000) used elastic stress analysis to predict saturation intensity of $D_s \approx 0.75$. Hobbs' model predicts $D_s \geq 2$ for unrealistic conditions in which the ductile layers are stronger by 20 times or more than the brittle one. In the next section, we present a new model for fracture intensity and fracture saturation for extensional tectonic regimes.

Fracture saturation in layered medium with frictional contacts

Approach

The present model is based on the analysis of Kelly and Tyson (1965) for composite material built of brittle fibers embedded in a ductile matrix. According to their concept, when a composite material is subjected to ex-

tension, the matrix extends by continuous flow, whereas the fiber extends elastically and by fracturing. When the composite is extended, the stress transfer from the matrix to a fiber is manifested by shear stresses along the contact between the two media. The higher tensile stresses in a fiber lead to its tensile fracturing, and the spacing between the fractures decreases until the fiber–matrix contact yields by shear. This yielding of the contact stops the fracturing of the fiber, and final fracture saturation is achieved. According to Kelly and Tyson (1965), the final fracture saturation depends on the tensile strength of the fiber and the shear strength of the contact surface.

We adopted the model of Kelly and Tyson (1965) because it fits well the fracturing processes of layered rocks, and because it requires the knowledge of only a few, well-bounded mechanical parameters. The layer contacts are regarded as frictional discontinuities, and it is assumed that their friction coefficient is 0.6–0.85, according to Byerlee’s law (Byerlee, 1978; Reches et al., 1992). Thus, the shear stresses along the layer contacts can be bounded if the depth and inclination of the layers are known.

Model Derivation

Kelly and Tyson (1965) used force balance to show that under tension the stress, $\sigma(x)$ at a distance x from the first fracture in the fiber, depends on the shear stress along the fiber contacts,

$$\sigma(x) = 2\tau_y \frac{x}{R} \quad (1)$$

where τ_y is the shear stress along the fiber (assumed to be uniform) and R is the fiber radius.

Eq 1 indicates that the tensional stress increases linearly with distance (x), yet its magnitude must be bounded by the tensile strength of the fiber, T . A new fracture is created in the fiber at a distance (x) in which $\sigma(x) = T$. Under increasing extension, this process continues to fracture the fiber with gradually decreasing spacing between the fractures (Fig. 1b). The distance between fractures reaches a critical distance, L_C , when the shear stress at the fiber contact is larger than the frictional strength of the contact, τ_{yc} , (Fig. 1b). According to eq 1, the fiber will be disconnected from the matrix when

$$L_C = R \frac{T}{2\tau_{yc}} \quad (2)$$

Equation 2 is the “Kelly Equation” (Roman et al., 1992), which predicts that fracture saturation intensity of the composite will occur in the range of $L_C/2 - L_C$ with a mean length value of

$$\langle L_M \rangle = \frac{3}{4} L_C \quad (3)$$

For the application of these concepts to the analysis of layered rock, we consider a 2D configuration with a sequence of two ductile layers with a brittle layer between them (Fig. 1a). The layers are horizontal with a remote stress state of $\sigma_v > \sigma_h$, where the vertical stress, σ_v , reflects the overburden load. Both remote stresses are compressive, such as is common in extensional tectonic regimes (Reches et al., 1992; Zoback, 1992). It is assumed here, similar to the model of Kelly and Tyson, that the extension of the ductile layers is continuous and larger than the extension of the brittle layer (see also Gross et al., 1995; Reches, 1998). This larger extension of the ductile layers invokes a shear stress τ_{xy} along the layer contacts that transfers load from the ductile layers to the brittle one.

Following our above assumption that the layer contacts behave as frictional rock interfaces, the shear stress along the contacts is

$$\tau_{xy} \leq a\sigma_v + b \quad (4)$$

where σ_v is the normal stress component (in our configuration $\sigma_n = \sigma_v$), and a , b are Byerlee’s coefficients of $a = 0.85$ and $b = 0$ at depth of 10 km or less. Applying the force balance concept (eq 1) to the present geometry, the horizontal stress within the brittle layer at distance x from an existing fracture is

$$\sigma(x) = 2\tau_{xy} \frac{x}{h} \quad (5)$$

Near the fracture surfaces, the tensile stresses and the shear stresses between the layers are \sim zero, and they increase linearly with distance (see above). A new fracture would form when

$$\sigma(x) = \sigma_h + T \quad (6)$$

where T is the tensional strength of the brittle layer. As the maximum shear stress at the layer contacts is bounded by the friction (eq 4), the critical length value (eq 2) can be determined by substituting eqs 4 and 5 in eq 6 and rearranging. We find that the critical fracture spacing is

$$L_C = \frac{h(\sigma_h + T)}{2(a\sigma_v + b)} \quad (7)$$

Taking $b = 0$ in the upper 10 km of the crust (Byerlee, 1978; Reches et al., 1992), and using eq 3 for the mean spacing, we find that the saturation intensity can be written as

$$D_S = \frac{8}{3} \frac{a\sigma_v}{\sigma_h + T} \quad (8)$$

Equation 8 presents the saturation fracture intensity as a function of the friction coefficient between layers (a), the tectonic stresses (σ_h), and the strength of the brittle layer (T). According to our model, the rise of extension after fracture saturation would lead to shear failure and slip along the layers' contacts; such slip will be similar to bedding-plane slip documented during folding (Ghosh, 1968; Reches and Johnson, 1976). It is thus expected that further extension will be accommodated by the opening of existing joints, and flow or fracture of the ductile layers (Becker and Gross, 1996).

MODEL APPLICATION TO THE DEAD SEA MARGINS

We apply the above model to joint intensity measurements in dolostone layers within the western margins of the Dead Sea (Sagy et al., 2001, 2003). The Dead Sea basin is bounded on its western margins by a belt of large, active faults. The belt trends N-S; it is 100 km long, 3–5 km wide, and the cumulative vertical displacement along its faults exceeds 10 km. Sagy (1999) used borehole image analysis and stress inversion methods to find that the stress field in this area is extensional with $\sigma_v > \sigma_H > \sigma_h$. We measured fractures in stations that are located on exposures of dolostone and limestone of the Judea Group, distributed along 50 km of the belt. The present analysis is limited only to systematic joint sets in the dolostone layers (17 stations). The studied fractures were recognized as joints by their fractographic features (Bahat, 1991): concentric rib marks, and radial plumose or hackle marks. Most of the measurements are based on mapping, at 1:10 scale, of joints exposed on top of sub-horizontal layers. In other sites, we used scan-lines that ran 30–120 m long (Sagy, 1999; Sagy et al., 2003).

Measurement in these 17 stations yielded 31 values of D , including 17 values for the dominant sets in each of the stations, and 14 values for the secondary sets. The plot of these data (Fig. 2a) reveals three distinct groups: Group A with $D = 1.3$ – 2.6 for the dominant joint set in thin layers ($h < 0.5$ m); Group B with $D < 1$ for the secondary joint set in thin layers ($h < 0.5$ m); and Group C with $D > 3$, for the layers with $h > 0.5$ m. Note that the highest intensity in Group A is in one station with $D = 3.5$, located a few meters from a large normal fault.

The expected saturation intensity in this area is calculated according to the above frictional model (eq 8) and the following parameters are estimated. First, it

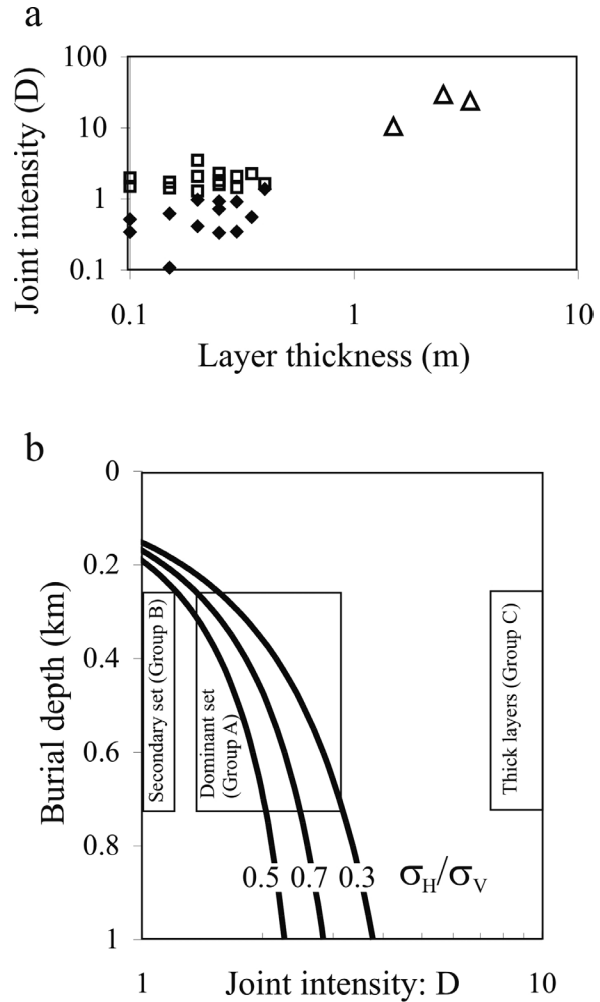


Fig. 2. Joint intensity in the western margins of the Dead Sea basin. (a) Measured joint intensity ($D = h/S_m$) in dolostone layers divided into three groups: Group A of dominant joint sets in layers of $h < 0.5$ m (open squares); Group B of secondary joint sets in the same layers (solid diamonds); Group C of joint sets in layers of $h > 0.75$ m (open triangles). (b) Predictions of the present model (see text) for the saturation joint intensity (D_s) in layered rocks as a function of the burial depth. Calculated for the parameters estimated for the western margin of the Dead Sea (see text): $T = 7.5$ Mpa, $a = 0.85$, and the marked curves of $\sigma_h/\sigma_v = 0.3, 0.5$, and 0.7 .

is assumed that the pore pressure is constant in all layers, and thus the tectonic stresses are regarded as the effective stresses. Second, we assume $\sigma_v = \rho gH$, where $\rho = 2,500$ kg/m³ is the mean rock density, g = gravitational acceleration, and $H = 0.3$ – 0.7 km is the depth range of the measured rock layers (Sagy, 1999). Third, following Byerlee's law we use $a = 0.85$ and b

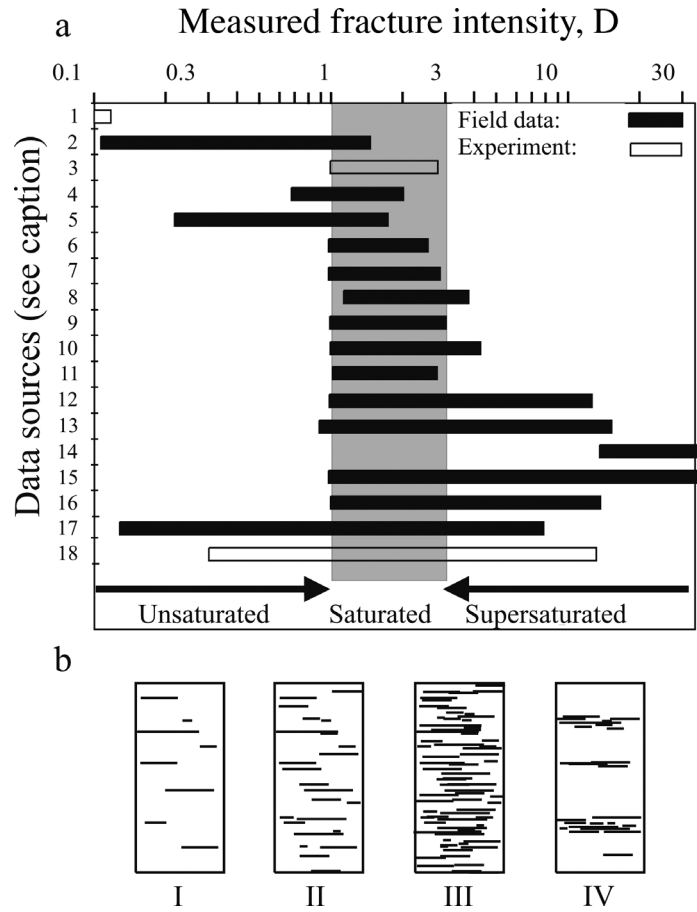


Fig. 3. (a) Measured joint and fracture intensity in field and experiments. Dotted zone at $1.0 < D < 3.0$ is the range of intensities predicted by the models (see text). Studies are divided into three groups, with $D < 3$ for the undersaturated group, $1 < D < 3$ for the saturated group, and $D > 3$ for supersaturated cases (see text). [Data sources: 1. Wu and Pollard (1995); 2. Narr and Suppe (1991); 3. Garrett and Bailey (1977); 4. Ji et al. (1998); 5. Engelder et al. (1997); 6. Gross et al. (1995); 7. Wu and Pollard (1995); 8. Narr and Suppe (1991); 9. Gross (1993); 10. Huang and Angelier (1989); 11. Price (1966); 12. McQuillan (1973); 13. Becker and Gross (1996); 14. Reches (1998); 15. Reches (1972); 16. Ladeira and Price (1981); 17–18. Sagy et al. (2001)]. (b) A scheme of the unsaturated (I), saturated (II), supersaturated (III), and clustered (IV) classes.

= 0. Fourth, we use tensile strength of $T = 7.5$ MPa for dolomite rocks (Finno, 2002). Finally, we assume that the range of tectonic stress ratio, σ_h/σ_v , is from 0.3 to 0.7, as shown for example by Reches et al. (1992) and Zoback (1992).

The predicted D_s for $\sigma_h/\sigma_v = 0.3-0.7$ (effective stresses) are plotted in Fig. 2b. The measured values of D (of groups A, B, and C) are also plotted as rectangles at the appropriate depth interval of H . This plot indicates a good agreement between measured D values and predicted D_s values: group A (the dominant joint set in each field station, Sagy, 1999) fits the corresponding saturated values for the marked conditions, and group B (the less-developed joint set) fits the

unsaturated range of D values. However, the intensity of group C, with $D = 8-22$, is supersaturated and cannot be explained by the present model or by any other quasi-static models.

CLASSES OF JOINT INTENSITY

Observational classes

The compilation of fracture intensity observations in the field and experiments reveals that D values range from 0.1 to 35 (Fig. 3a). On this range of observed D values, we plot the band of predicted saturation intensity as $D_s = 1.0-3.0$, which encompasses the model predictions for a reasonable range of rock proper-

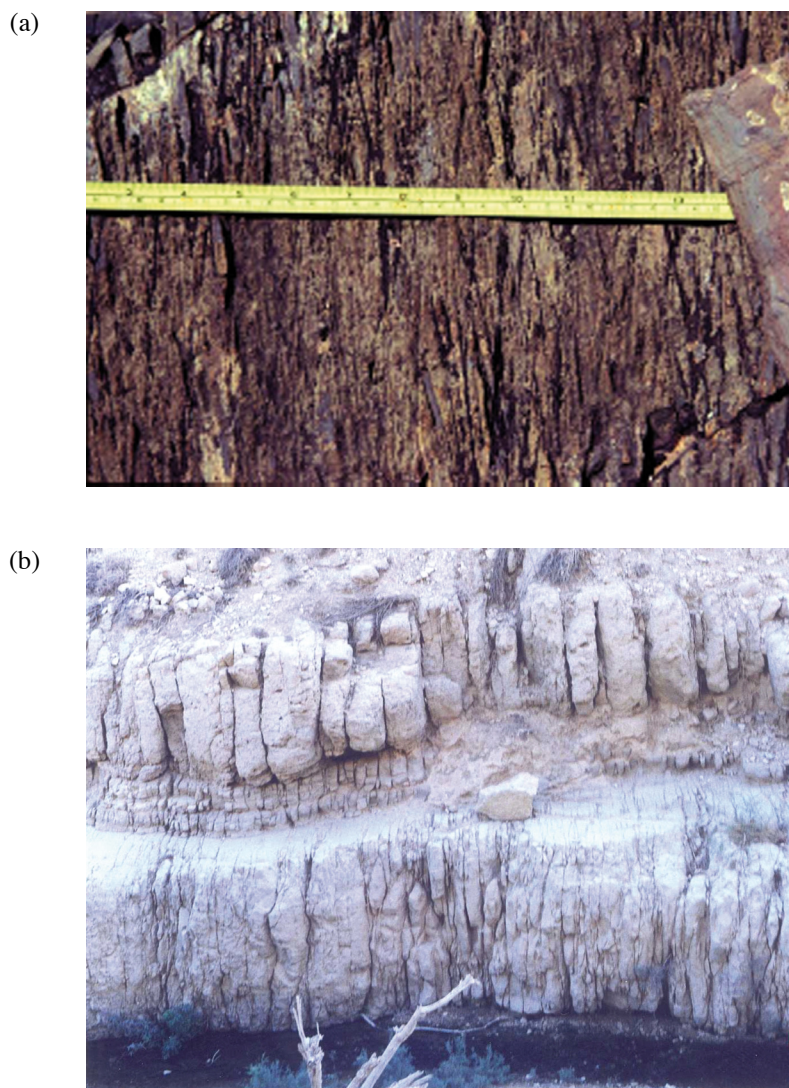


Fig. 4. Field examples for supersaturated jointing in layered carbonate rocks. (a) Joints observed on the upper surface of limestone layer, Carmel Formation, Cedar Mountain, Utah, with width $h = 0.1$ m and mean spacing $S_m \approx 3$ mm, and $D \approx 33$. (b) View of joints in dolomite layers, Ein Gedi area, western margin of the Dead Sea basin. The mean spacing in the 3.0-m-thick bottom layer is ≈ 0.15 m.

ties. This band divides the observed data into three intensity classes (Fig. 3a), which are portrayed schematically in Fig. 3b. These classes are (1) unsaturated with $D < 1.0$, (2) saturated with $D = 1.0-3.0$, and (3) supersaturated with $D > 3.0$. A fourth class, which was termed clustered (Sagy et al., 2001), or swarm (Putot et al., 2001) is displayed in Fig. 3b; this class has irregular intensity with local $D > 3.0$ and mean $D < 3.0$. These four classes are characterized below by several examples.

The saturated and unsaturated classes

Our observations of group A (Fig. 2a) join many previous field observations that demonstrated a linear relationship between layer thickness and mean joint spacing, and model-predicted joint intensity. These relations are common for thin layers in many tectonic regimes and for a range of sedimentary rocks (Ladeira and Price, 1981; Ji et al., 1998). The mean D value in our results is larger than observed in other tectonic

regimes (e.g., Narr and Suppe, 1991; Gross, 1993). These variations can reflect the different measuring methods (Wu and Pollard, 1995), or different values of the σ_h/σ_v ratio for other tectonic regimes. Furthermore, joint interaction and rise of pore pressure, even under extensional load, could raise the local values of σ_h and prevent further jointing (Bai and Pollard, 2000; Germanovich and Astakhov, 2004).

The unsaturated class is represented here by secondary joint systems. In general, this class could include any joint set that is only partly developed due to low extension intensity.

The supersaturated class, field examples

Three cases of supersaturated fracture intensity are presented below. One case is in thick layers (McQuillan, 1973; Ladeira and Price, 1981), a second is in thin layers (Reches, 1998), and a third is of gradual systematic intensity increase within one layer in the proximity of a fault (Sagy et al., 2001).

McQuillan (1973) analyzed joint sets of Asmari Limestone in southwest Iran, an intensely folded region with Mesozoic thrust systems. He used the scan-line method to measure joint intensity in hundreds of stations within a 320-km-long region. McQuillan (1973) found that joint spacing is nonlinearly related to layer thickness and that the associated D values are as high as $D \approx 11$ in 12-m-thick layers. He also noted that joint intensity in the Asmari Limestone does not depend on local folding, and that very tight joints were observed in graben regions where fault-associated joints predominate. Ladeira and Price (1981) presented similar intensity relations for graywacke and sandstone layers in England and Portugal. Their results indicate D values up to 35 in layers thicker than 0.5 m.

Reches (1998) studied the joints within limestone layers of the Carmel Formation, Cedar Mountain area, central Utah (Fig. 4a). These are flat-lying layers in the Colorado Plateau region, east of the San Raphael swell. The limestone layers are 0.05–0.75 m thick and are embedded between much thicker layers of compliant siltstone, marls, and shales. The limestone layers are intensely fractured by two dominant sets of sub-vertical joints; the angle between the strikes of the two sets is about 40° . The fracture intensity was measured using the scale-line method on horizontal or vertical surfaces, and in the cumulative-length method for maps; the calculated D values range from 3 to 34.

Sagy et al. (2001) mapped joints within a 3-m-thick layer of brittle dolomite in the Ein Gedi area, the west

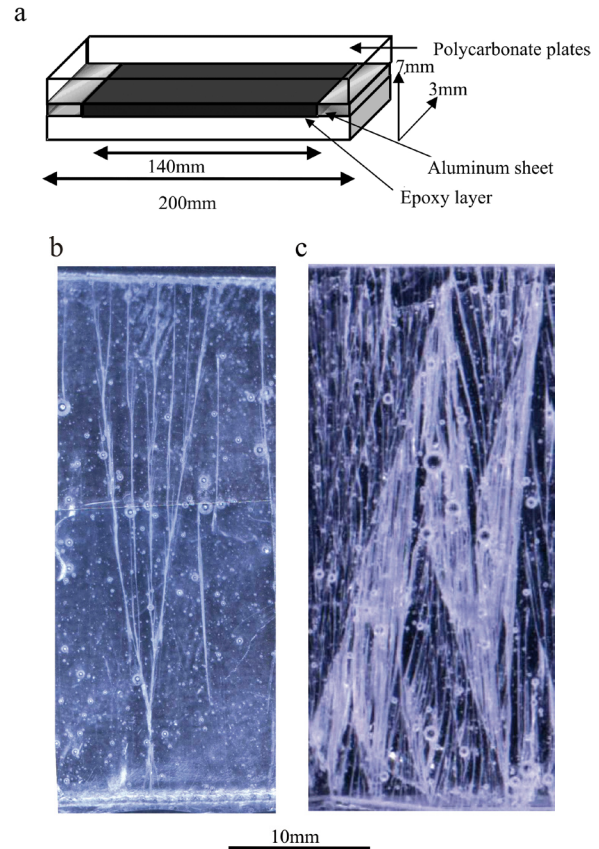


Fig. 5. Experimental fracturing in layered composites subjected to layer-parallel extension (after Sagy, 1999). (a) Sample set-up that includes a brittle epoxy layer (1 mm thick) that cements two thick polycarbonate plates (each 3 mm thick). External dimensions are $200 \times 30 \times 7$ mm; Aluminum spacers replace the epoxy where the loading frame grippers are tightened on the sample. (b–c) Map view of the tensile fractures (bright lines) in the epoxy layer as observed through the transparent polycarbonate layer; extension is horizontal. (b) Close-up view of a single branching fracture. (c) Close-up view of a single clustering fracture. The final density of $D \approx 10$ results from the high density inside the clusters and partly overlaps between clusters.

margins of the Dead Sea (Fig. 4b). The dolostone layer is exposed along a 120-m-long sub-vertical erosional wall that was mapped at scales from 1:20 to 1:1. This exposure is bounded on the east side by a large normal fault that displaced the mapped layer by at least tens of meters. The intensity of the large joints in the exposure increases significantly toward the fault. While $D \approx 2.0$ at a distance of 80–100 m west of the fault, it increases to $D \approx 22$ at 30 m distance from the fault (Sagy et al.,

2001). Detailed mapping revealed that most of the joints have a “tree-like” shape with many branches. These branches increase the surface area of a single joint by a factor of ten or more (Sagy et al., 2001). In the proximity of the fault, the branches of neighboring joints create a dense fracture network within a fragmented layer.

Supersaturated and clustered classes in laboratory experiments

Laboratory experiments with layered composites usually yielded low values of saturation densities. Garrett and Bailey (1977) stretched a layered composite of fibers within resin and demonstrated that D increases with extension until the samples failed when D approached 1.0. Wu and Pollard (1995) bent ductile plates with thin brittle coating, and the maximum achieved intensity approached $D = 0.15$. In contrast to these experiments, our tests (Sagy, 1999; Sagy et al., 2001) generated high saturation densities of $D \leq 10$. We used layered composites made of two polycarbonate layers cemented to each other by brittle epoxy and subjected to axial extension (Fig. 5a). All four classes of fracture intensity were observed in these experiments (Sagy, 1999). We present here, however, only tests in which the epoxy behaved in a brittle mode (when the strain rates were higher than $1 \cdot 10^{-3} \text{ s}^{-1}$; Sagy et al., 2001). We describe only tests with branching fractures and tests with fracture intensity of the clustered class.

The experimental branching fractures (Fig. 5b) are composed of many short segments that split from each other with up to six forking segments at a single junction. Branches form a hierarchical structure with up to eight branching levels in the present experiments. The measured cumulative length of all observed branches in a single fracture is up to six times the length of a planar fracture across the sample.

Clustering fractures (Fig. 5c) developed under the highest strain rates of these tests, with extension rates of $2 \cdot 10^{-3} \text{ s}^{-1}$ to $7 \cdot 10^{-3} \text{ s}^{-1}$. A clustering fracture includes several branching fractures that crosscut each other, forming a wide zone of intense fracturing. In a simple cluster each branch may be traced to its parent fracture, but complex clusters appear as integral structural units of intensely fractured zones (Fig. 5c). Further, the experiments indicate that a clustering fracture grows during a single, fast event (Sagy et al., 2001). Video records of the tests show that in a 30-mm-wide sample a cluster develops in less than 0.04 s (Reches et al., 2000). While all fractures inside one cluster develop quasi-simultaneously, whole clusters continue to

fill the sample gradually as long as the axial extension increases (Reches et al., 2000). Clustering stopped due to delamination or yielding of the polycarbonate layers.

A cluster or a branching fracture includes many secondary segments with large cumulative length and enlarged surface area with respect to a planar fracture. The global fracture intensity for several clusters has two contributions: (1) the cumulative length of the fractures inside the cluster, L_p , and (2) the number of clusters, n . The fracture intensity determined in the cumulative-length method for a sample with area A is:

$$D = h (n \cdot L_p / A)$$

Our measurements inside individual clusters indicate local D values in the range of 5–13, whereas the corresponding D of the entire sample is 2.5–10. These values are about ten times higher than intensity values observed in our lower strain rate tests.

DISCUSSION

Saturation of natural joints

Models of fracture intensity in layered media or composite materials suggested that the intensity should exhibit a saturation limit. First, the ductile layers can fail (Hobbs, 1967). Second, the brittle layer can be delaminated from the ductile layers, if the shear stresses along the layers' contacts exceed the contact shear strength (or the ductile layers' strength) (Kelly and Tyson, 1965; Garrett and Baily, 1977). Third, the existing fractures induce compressive stresses between themselves and prevent further fracturing of the brittle layer (Bai and Pollard., 2000; Germanovich and Astakhov, 2004). Based on the present compilation of field measurements (Figs. 2a,3a) and the results of our model (Fig. 2b), we suggest that saturation intensities for realistic geological cases converge to the range of $D_s = 0.75\text{--}3.0$. The same compilation, however, suggests that this range is relatively small with respect to the range of intensities, $D_s = 0.1\text{--}35$, observed in the field. We classify above the four classes of joint intensity (Figs. 2, 3): unsaturated ($D < 1.0$), saturated ($D = 1.0\text{--}3.0$), supersaturated ($D > 3.0$), and clustered of irregular intensity with local $D > 3.0$ and mean $D < 3.0$. Apparently, the above outlined models cannot explain the supersaturated class that is found in various geological settings. A possible mechanism that could fracture the layer at supersaturated intensity is outlined below.

Mechanisms of high-density fracturing

Dynamic fracturing is a nonlinear process in which a tensile fracture propagates at high velocities that approach the Raleigh wave velocity, V_R , of the host material (Freund, 1990). Dynamic fracturing is associated with high fracture intensity, branching, and clustering of the fractures (Sharon and Fineberg, 1996; Fineberg and Marder, 1999; Sagy et al., 2001). These features indicate that high intensity of fractures could reflect the profound increase in cumulative length (= surface area) of the secondary fractures within individual branched fractures. As the cumulative fracture length is increased by a factor of ten or more inside a cluster (see above), we anticipate that a complete “filling” of a layer by clusters (e.g., Reches et al., 2000) would generate a similar increase of the global intensity (Sagy et al., 2001). Although dynamic fracturing proved to be an effective mechanism to create dense fractures and clusters, it is probably limited to specific tectonic conditions, for example, near large faults (Sagy et al., 2001) or at impact sites (Sagy et al., 2004). These high-energy environments could supply the energy that is required to create large branches and dynamic fractures.

Another mechanism for supersaturated tensile fractures and swarms was suggested by Germanovich and Dyskin (2000), who showed that high fracture intensity could be induced by an extensional state of stress that develops near the free boundary, when $\sigma_h \ll \sigma_v$. The dynamic fracturing as well as the Germanovich and Dyskin (2000) model, which allow for $D \gg 1$, assume elastic rheology. Yet, the anomalous high joint intensity in thick layers cannot be easily explained by either of these two mechanisms, and further research is required to solve this enigma.

ACKNOWLEDGMENTS

This paper is dedicated to the memory of Dr. Nachman Schulman, the Structural Geology teacher and M.Sc. advisor of the second author (Z.R.). Nachman combined encyclopedic knowledge and a didactic approach that made him a critical listener and an outstanding teacher. Thanks, Nachman.

Discussions with Jay Fineberg, Izhak Roman, Gil Cohen, and Shmuel Rubinstein are greatly appreciated. The reviews by Amotz Agnon and Yossi H. Hatzor significantly improved the manuscript. The study was supported by the United States-Israel Binational Science Foundation (Grant 98-135), and the Israel Science Fund (Grant 175-02).

REFERENCES

- Bahat, D. 1991. Tectonofractography. Springer-Verlag, Berlin, 354 pp.
- Bai, T., Pollard, D.D. 2000. Fracture spacing in layered rocks: a new explanation based on stress transition. *J. Struct. Geol.* 22: 43–57.
- Becker, A., Gross, M.R. 1996. Mechanism for joint saturation in mechanically layered rocks: an example from southern Israel. *Tectonophysics* 257: 223–237.
- Byerlee, J.D. 1978. Friction of rocks. *Pure Appl. Geophys.* 116: 615–626.
- Engelder, T., Gross, M.R., Pinkerton, P. 1997. An analysis of joint development in thick sandstone beds of Elk basin anticline, Montana-Wyoming. In: Hoak, T.E., Klawitter, A.L., Blomquist, P.K., eds. *Fractured reservoirs: characterization and modeling*. Rocky Mtn. Assoc. Geol., pp. 4–21.
- Fineberg, J., Marder, M. 1999. Instability in dynamic fracture. *Phys. Rep.* 313: 2–108.
- Finno, R.J. 2002. Evaluation of capacity of micropiles Embedded in dolomite. Tech. Rep. No. A433, Northwestern Univ., Chicago.
- Freund, L.B. 1990. *Dynamic fracture mechanics*. Cambridge Univ. Press, Cambridge, 563 pp.
- Garrett, K.W., Baily, J.E. 1977. Multiple transverse fracture in 90° cross-ply laminates of a glass-reinforced polyester. *J. Mater. Sci.* 12: 157–168.
- Germanovich, L.N., Dyskin, A.V. 2000. Fracture mechanisms and instability of openings in compression. *Int. J. Rock Mech. Min.* 37: 263–284.
- Germanovich, L.N., Astakhov, D.K. 2004. Stress-dependent permeability and fluid flow through parallel joints *J. Geophys. Res.* 109 (B9): Art. No. B09203.
- Ghosh, S.K. 1968. Experiments of buckling of multilayers which permit interlayer gliding. *Tectonophysics* 6: 207–249.
- Gross, M.R. 1993. The origin and spacing of cross joints; examples from the Monterey Formation, Santa Barbara coastline, California. *J. Struct. Geol.* 15: 737–751.
- Gross, M.R., Fischer, M.P., Engelder, T., Greenfield, R.J. 1995. Factors controlling joint spacing in interbedded sedimentary rocks; integrating numerical models with field observations from the Monterey Formation, USA. In: Ameen, M.S., ed. *Fractography: fracture topography as a tool in fracture mechanics and stress analysis*. Geol. Soc. Spec. Pub. Vol. 92, pp. 215–233.
- Hobbs, D.W. 1967. The formation of tension joints in sedimentary rocks; an explanation. *Geol. Mag.* 104: 550–556.
- Huang, Q., Angelier, J. 1989. Fracture spacing and its relation to bed thickness. *Geol. Mag.* 126: 353–362.
- Ji, S., Zhu, Z., Wang, Z. 1998. Relationship between joint spacing and bed thickness in sedimentary rocks: effects of interbed slip. *Geol. Mag.* 135: 637–655.
- Kelly, A., Tyson, W.R. 1965. Tensile properties of fiber-rein-

- forced metals: copper/tungsten and copper/molybdenum. *J. Mech. Phys. Solids* 13: 329–350.
- Ladeira, F.L., Price, N.J. 1981. Relationship between fracture spacing and bed thickness. *J. Struct. Geol.* 3: 179–183.
- McQuillan, H. 1973. Small-scale fracture density in Asmari Formation of southwest Iran and its relation to bed thickness and structural setting. *Am. Assoc. Petrol. Geol. Bull.* 57: 2367–2385.
- Narr, W., Suppe, J. 1991. Joint spacing in sedimentary rocks. *J. Struct. Geol.* 13: 1037–1048.
- Price, N.J. 1966. *Fault and joint development in brittle and semi-brittle rock.* Pergamon Press, Oxford, England, 176 pp.
- Putot, C., Chastanet, J., Cacas, M.C., Daniel, J.M. 2001. Fractography in sedimentary rocks: tension joints sets and fracture swarms. *Oil Gas. Sci. Technol.* 56: 431–449.
- Reches, Z. 1972. Jointing in the Hazera and Hathira monoclines, northern Negev. M.Sc. thesis, Hebrew Univ., Jerusalem (in Hebrew, English abstr.).
- Reches, Z. 1998. Tensile fracturing of stiff rock layers under triaxial compressive stress states. *J. Rock Mech. Min. Sci.* 35: 456–457.
- Reches, Z., Johnson, A.M. 1976. A theory of concentric, kink and sinusoidal folding and of monoclinial flexuring of compressible, elastic multilayers; VI, Asymmetric folding and monoclinial kinking. *Tectonophysics* 35: 295–334.
- Reches, Z., Baer, G., Hatzor, Y. 1992. Constraints on the strength of the upper crust from stress inversion of fault slip measurements, *J. Geophys. Res.* 97: 12,481–12,493.
- Reches, Z., Sagy, A., Roman, I. 2000. Dynamic fracturing web page at: <http://earth.es.huji.ac.il/reches/dynamic/>
- Roman, I., Krishnamurthy, S., Miracle, D.B. 1992. Interfacial shear properties and acoustic emission behavior of model aluminum and titanium matrix composites. Proc. 4th Int. Symposium on Acoustic Emission in Composite Materials, ASNT, Seattle, pp. 109–114.
- Sagy, A. 1999. Jointing and faulting processes along the western margins of the Dead Sea basin. M.Sc. thesis, Hebrew Univ., Jerusalem, 45 pp. (in Hebrew, English abstr.).
- Sagy, A., Reches, Z., Roman, I. 2001. Dynamic fracturing: field and experimental observations. *J. Struct. Geol.* 23: 1223–1239.
- Sagy, A., Reches, Z., Agnon, A. 2003. Hierarchic 3D architecture and mechanics of the margins of the Dead Sea pull-apart. *Tectonics* 22: 1, TC001323.
- Sagy, A., Fineberg, J., Reches, Z. 2004. Shatter cones: rapid branched fractures formed by shock impact. *J. Geophys. Res.* 109, (B10) 209, 20 pp.
- Sharon, E., Fineberg, J. 1996. Microbranching instability and the dynamic fracture of brittle materials. *Phys. Rev.* 54: 7128–7139.
- Sowers, G.M. 1973. Theory of spacing of extension fracture. *Eng. Geol. Case Hist.* 9: 27–53.
- Wu, H., Pollard, D.D. 1995. An experimental study of the relationship between joint spacing and layer thickness. *J. Struct. Geol.* 17: 887–905.
- Zoback, M.L. 1992. 1st-order and 2nd-order patterns of stress in the lithosphere—the world stress map project. *J. Geophys. Res.* 97: 11703–11728.



Columnar basalt. Photo: N. Schulman.